

Published in final edited form as:

DNA Repair (Amst). 2013 May 1; 12(5): 377–388. doi:10.1016/j.dnarep.2013.02.008.

## Mouse DNA Polymerase Kappa Has A Functional Role In the Repair of DNA Strand Breaks

Xiuli Zhang<sup>1,\*</sup>, Lingna Lv<sup>1,\*</sup>, Qian Chen<sup>2,\*</sup>, Fenghua Yuan<sup>3</sup>, Ting Zhang<sup>1</sup>, Yeran Yang<sup>1</sup>, Hui Zhang<sup>1</sup>, Yun Wang<sup>2</sup>, Yan Jia<sup>1</sup>, Liangyue Qian<sup>3</sup>, Benjamin Chen<sup>4</sup>, Yanbin Zhang<sup>3</sup>, Errol C. Friedberg<sup>5</sup>, Tie-Shan Tang<sup>2,#</sup>, and Caixia Guo<sup>1,#</sup>

<sup>1</sup>Laboratory of Cancer Genomics and Individualized Medicine, Beijing Institute of Genomics, Chinese Academy of Sciences, Beijing 100101, China

<sup>2</sup>State Key Laboratory of Biomembrane and Membrane Biotechnology, Institute of Zoology, Chinese Academy of Sciences, Beijing 100101, China

<sup>3</sup>Department of Biochemistry & Molecular Biology, University of Miami Miller School of Medicine, Miami, FL 33136

<sup>4</sup>Division of Molecular Radiation Biology, Department of Radiation Oncology, University of Texas Southwestern Medical Center, Dallas, TX 75390, USA

<sup>5</sup>Department of Pathology, University of Texas Southwestern Medical Center, Dallas, TX 75390, USA

### Abstract

The Y-family of DNA polymerases support of translesion DNA synthesis (TLS) associated with stalled DNA replication by DNA damage. Recently, a number of studies suggest that some specialized TLS polymerases also support other aspects of DNA metabolism beyond TLS *in vivo*. Here we show that mouse polymerase kappa (Pol $\kappa$ ) could accumulate at laser-induced sites of damage *in vivo* resembling polymerases eta and iota. The recruitment was mediated through Pol $\kappa$  C-terminus which contains the PCNA-interacting peptide, ubiquitin zinc finger motif 2 and nuclear localization signal. Interestingly, this recruitment was significantly reduced in MSH2-deficient LoVo cells and Rad18-depleted cells. We further observed that Pol $\kappa$ -deficient mouse embryo fibroblasts were abnormally sensitive to H<sub>2</sub>O<sub>2</sub> treatment and displayed defects in both single-strand break repair and double-strand break repair. We speculate that Pol $\kappa$  may have an important role in strand break repair following oxidative stress *in vivo*.

### Keywords

Polymerase kappa; PCNA; MSH2; strand break repair; laser micro-irradiation

---

© 2013 Elsevier B.V. All rights reserved.

#Authors to whom correspondence should be addressed: guocx@big.ac.cn, tangtsh@ioz.ac.cn.

\*Equal contributions

### Conflict of Interest statement

The authors declare no competing interests.

**Publisher's Disclaimer:** This is a PDF file of an unedited manuscript that has been accepted for publication. As a service to our customers we are providing this early version of the manuscript. The manuscript will undergo copyediting, typesetting, and review of the resulting proof before it is published in its final citable form. Please note that during the production process errors may be discovered which could affect the content, and all legal disclaimers that apply to the journal pertain.

## 1. Introduction

Translesion DNA synthesis (TLS) is a mode of DNA damage tolerance, which utilizes specialized DNA polymerases to support DNA synthesis past a spectrum of template strand base damage [1]. Ten different such DNA polymerases have been shown to support TLS in mammalian cells *in vitro*. These enzymes are devoid of 3' → 5' proofreading exonuclease activity and replicate undamaged DNA *in vitro* with low fidelity and weak processivity [2]. Among them, DNA polymerases kappa (Polκ), iota (Polι), eta (Polη) and REV1 belong to a novel DNA polymerase family (the Y-family) [3,4]. In comparison with Polη and Polι, Polκ is the most resistant to bulky guanine N<sup>2</sup>-adducts and the most quantitatively efficient in catalyzing dCTP incorporation opposite bulky guanine N<sup>2</sup>-adducts, particularly the largest (N<sup>2</sup>-BPDE-dG) (a benzo[a]pyrene diolepoxide-N<sup>2</sup>-deoxyguanosine adduct) [5]. Consistently, Polκ-deficient cells are hypersensitive to BPDE and estrogen [6–9].

In addition to their involvement in TLS a number of studies suggest that some (if not all) specialized DNA polymerases support other aspects of DNA metabolism *in vivo* [10]. Polθ (an A-family DNA polymerase), Polζ (a B-family DNA polymerase) and Polι, Polη and REV1 have been implicated in somatic hypermutation and class switching associated with the maturation of antibody affinity [11]. Additionally, it has been reported that Polη can synthesize DNA from D-loop recombination intermediates when an invading DNA strand serves as the primer [12]. Polι has also been reported to have functions in base excision repair (BER) [13]. Human MRC5 fibroblasts with stably down-regulated Polι protein exhibit sensitivity to the DNA-damaging agent H<sub>2</sub>O<sub>2</sub> [13].

Polκ has been implicated in repair synthesis of DNA during nucleotide excision repair (NER) under some conditions [14], which might explain the UV sensitivity of Polκ-deficient cells [7,15]. More recently, Polκ protein displayed a high accuracy during dinucleotide microsatellite DNA synthesis *in vitro* [16] and played a role in limiting the rate of spontaneous germline mutation within two expanded short tandem repeat alleles in mice [17]. To explore whether Polκ will be analogous to Polι and Polη in the recruitment to laser-induced sites of damage and in protection of cells from oxidative damage [13,18], GFP-Polκ was expressed in cells and its accumulation at sites of damage was examined. Here, we showed that Polκ protein accumulated at sites of DNA damage in cells exposed to focal laser micro-irradiation, a well-characterized source of DNA strand breaks. This recruitment was significantly reduced in MSH2-deficient cells and Rad18-depleted cells. Moreover, Polκ-deficient mouse embryo fibroblasts (MEFs) exhibited an enhanced sensitivity to killing by the DNA-damaging agent H<sub>2</sub>O<sub>2</sub> and reduced rates of DNA strand break repair after H<sub>2</sub>O<sub>2</sub> treatment as measured by alkaline comet assay. Consistent with these observations, single-strand break repair (SSBR)/BER activity was reduced in extracts from Polκ-deficient cells. In addition, a defect in double-strand break repair (DSBR) was also detected in Polκ-deficient cells as manifested with a slower rate of γ-H2AX loss after H<sub>2</sub>O<sub>2</sub> treatment compared to wild-type (WT) control.

## 2. Materials and Methods

### 2.1. Plasmids

Full-length and a panel of truncated Polκ cDNAs were PCR amplified and cloned into pEGFP-C3 (Clontech) to generate enhanced green fluorescent protein (eGFP) fusion proteins as previously described [19]. DsRed-XRCC1 plasmid was a kind gift from Dr. David Chen, UT Southwestern Medical Center. Flag-MSH2 plasmid was a kind gift from Dr. Haiying Hang, Institute of Biophysics, Chinese Academy of Sciences. The human shRNA-Rad18 plasmids (TRCN0000003468 and TRCN0000003470) and a non-targeting control plasmid (shRNA-SHC002) were purchased from Open Biosystems.

## 2.2. Cells and reagents

Pol $\kappa$ -deficient (*Polk*<sup>-/-</sup>) MEFs were prepared as previously described[19]. XPC and Pol $\kappa$  double knockout (*Polk*<sup>-/-</sup>*Xpc*<sup>-/-</sup>) and XPC-deficient/Pol $\kappa$  wild-type (*Polk*<sup>+/+</sup>*Xpc*<sup>-/-</sup>) MEFs were derived from Day 14 embryos produced by mating male and female *XPC*-deficient/*POLK*-heterozygous mice, developed by breeding heterozygous *POLK* mice with the *XPC* knock-out mice[15,20]. Cell genotypes were confirmed by PCR. The early passage cells were immortalized with a simian virus 40 (SV40) large T-antigen expression vector. Pol $\kappa$ -deficient cells reconstituted with GFP-tagged mouse *POLK* cDNA were generated by retrovirus infection. The cDNA was subcloned into retroviral vector pMSCV-puro (Clontech, Mountain View, CA) and transfected into 293T cells to produce viral particles. Pol $\kappa$ -deficient MEFs were infected with viruses followed by puromycin selection, and the corrected clones were picked and expression of GFP-Pol $\kappa$  was confirmed by western blotting with anti-GFP antibody and fluorescent microscopy. U2OS cells were maintained in Dulbecco Modified Eagle medium (DMEM) supplemented with glutamax (Invitrogen) and 10% fetal bovine serum, 100 U/ml penicillin and 100  $\mu$ g/ml streptomycin under 5% CO<sub>2</sub>. Stable shRNA knockdown clones were generated by infecting U2OS cells with polybrene-supplemented medium obtained from 293T packaging cells transfected with the shRNA-Rad18 or shRNA-SHC002. Individual clones were isolated by limiting dilution in media containing puromycin (1  $\mu$ g/mL) and screened for Rad18 expression levels with antibodies against Rad18 (Abcam). The clones were irradiated with 15 J/m<sup>2</sup> of UVC and chromatin-fractions were harvested 6 h later as reported before[21]. The levels of PCNA monoubiquitination were examined with an anti-PCNA antibody (Santa Cruz). HCT116 and LoVo cells were obtained from ATCC. These cells were grown in Dulbecco Modified Eagle medium (DMEM) supplemented with glutamax (Invitrogen) and 10% fetal bovine serum. The SV40-transformed human fibroblast line MRC5 was kindly provided by Alan R. Lehmann, University of Sussex. MRC5 cells were transfected with a panel of truncated mouse pEGFP-Pol $\kappa$  constructs using Fugene 6 (Roche) according to the manufacturer's protocol. About 40 h later, the cells were micro-irradiated and processed for immunofluorescence as described below.

## 2.3. Laser micro-irradiation and imaging

DNA strand breaks were introduced in the nuclei of cultured cells by micro-irradiation with a pulsed nitrogen laser (Spectra-Physics; 365 nm, 10 Hz pulse) as previously described[22]. The laser system was directly coupled (Micropoint Ablation Laser System; Photonic Instruments, Inc.) to the epifluorescence path of the microscope (Axiovert 200M [Carl Zeiss MicroImaging, Inc.] for time-lapse imaging and focused through a Plan-Apochromat 63 $\times$ /NA 1.40 oil immersion objective (Carl Zeiss MicroImaging, Inc.). The output of the laser power was set at 58–70% of the maximum as indicated. During micro-irradiation and imaging, the cells were maintained at 37°C in 35-mm glass-bottom culture dishes (MatTek Cultureware). The growth medium was replaced by CO<sub>2</sub>-independent medium (Invitrogen) before analysis.

## 2.4. Immunofluorescence

Cells were cultured on glass coverslips. Before fixing in 4% paraformaldehyde, the cells were washed in phosphate buffered saline (PBS) once. For  $\gamma$ H2AX staining, samples were treated with 0.5% Triton X-100 for 15 min followed by blocking with 5% fetal bovine serum and 1% goat serum for 1 h. After the block, cells were incubated with anti- $\gamma$ H2AX (Millipore) for 45 min. For cyclobutane pyrimidine dimers (CPDs) staining, samples were treated with 0.5% Triton X-100 for 5 min and then denatured with HCl for 30 min. After blocking with 20% FBS for about 30 min, the samples were incubated with anti-CPDs (Cosmo Bio Co) for 45 min according to the manufacturer's protocol. Then the samples were washed three times with PBS and incubated with the appropriate secondary goat anti-

mouse Alexa Fluor dye conjugated secondary antibody (Molecular Probes) for 45 min. The cells were then washed with PBS, counterstained with DRAQ5 to visualize nuclear DNA as described previously. Images were acquired with a Nikon Eclipse TE2000-U confocal laser scanning microscope (Nikon Inc.) and processed with Adobe Photoshop 7.0.

## 2.5. Western blot analyses

MRC cells were treated with hydrogen peroxide (H<sub>2</sub>O<sub>2</sub>) in serum-free medium for 1 h at 4°C. Chromatin-fractions were harvested as previously described[23]. Samples were separated by SDS-PAGE and detected by immunoblotting with antibodies against PCNA or GFP (Santa Cruz).

## 2.6. Cell survival assays

Cells were seeded into 60 cm dishes (~200 cells/dish) in triplicates and allowed to adhere overnight. The cells were then treated with the indicated amount of hydrogen peroxide (H<sub>2</sub>O<sub>2</sub>) for 1 h at 4°C in serum-free medium and were washed twice and further incubated in complete medium for 7–10 days. Colonies were fixed and counted. Survival fraction is calculated as number of colonies in the test condition/number of colonies in the control and plotted percentage against H<sub>2</sub>O<sub>2</sub> concentration. All experiments were carried out in triplicate. Data points are indicated as mean with standard error.

## 2.7. Comet assay

The alkaline comet assay was carried out as before [24] with some modification. Briefly, cells were treated with indicated amount of H<sub>2</sub>O<sub>2</sub> at 4 °C for 10 min or 300 μM methyl methanesulfonate (MMS) for 1 h, washed and reincubated in normal media for indicated time before processing. Harvested cells (1 × 10<sup>4</sup>) were mixed with 0.5% low melting agarose and layered onto agarose-coated slides. Slides were then submerged into cold lysis buffer [2.5 M NaCl, 100 mM EDTA, 10 mM Tris (pH 10.0), 1% N-lauroylsarcosine and 1% Triton X-100] for 1 h at 4°C. After lysis, slides were incubated for 20 min in electrophoresis buffer (300 mM NaOH and 1 mM EDTA, pH >13). After electrophoresis (20 min, 25 V, 300 mA), slides were neutralized with 0.4 M Tris, pH 7.5, for 30 min, placed into 100% ethanol and then air-dried. Slides were subsequently stained with 5 μg/ml ethidium bromide (Sigma) and images were taken using a fluorescent microscope (Leica). Average Olive Tail Moment (OTM) was analyzed (100 cells/slide) by using Comet Assay Software Project Casp-1.2.2 (University of Wroclaw, Poland). All experiments were repeated more than three times. The reported OTMs were the mean values ± standard deviation (S.E.) of three independent experiments.

## 2.8. *In vitro* BER assay using oligonucleotide substrate

Cell-free MEF extracts were prepared essentially as previously described [18], aliquoted, and stored at –80°C. *In vitro* BER assay was performed using the same oligonucleotide substrate as described by Petta et al [13]. Briefly, a 40-mer DNA substrate 5′-GTGGCGCGGAGACTTAGAGAUATTTGGCGCGGGGAATTCC-3′ containing uracil and complementary strand with G opposite uracil at a final concentration of 4 nM was incubated with 10 μg of MEF cell-free extract in 50 mM Hepes-KOH (pH 7.5), 5 mM MgCl<sub>2</sub>, 20 mM NaCl, 0.5 mM DTT, 4 mM ATP, 20 μM of each dATP, dGTP, and dTTP, and 0.33 μM [α-<sup>32</sup>P]dCTP at 37°C for the indicated time as described previously [13]. Reaction products were resolved by electrophoresis in denaturing 10% polyacrylamide gels (Acr:Bis = 19:1) in 0.5X TBE and visualized with a X-ray film. Repair of the uracil was evaluated by measuring the appearance of [α-<sup>32</sup>P]-labeled 40 mer oligonucleotide on the gel.

### 3. Results

#### 3.1. Accumulation of GFP-Pol $\kappa$ at laser-induced DNA lesions

It has been shown that Pol $\nu$  and Pol $\eta$  can be recruited to laser-induced sites of damage and protect cells from oxidative damage. To check whether Pol $\kappa$  behaves similarly, MRC cells expressing GFP-Pol $\kappa$  were exposed to laser micro-irradiation. The selective use of energy outputs known to generate both SSB and DSB revealed the selective accumulation of GFP-Pol $\kappa$  at radiation tracks (Fig. 1A). Additionally, we observed colocalization of GFP-Pol $\kappa$  with  $\gamma$ H2AX (Fig. 1B) and XRCC1 (Fig. 1C) proteins, distinctive “markers” of DSB and SSB respectively. Unlike XRCC1 whose localization to the laser damage sites is fast and transient, GFP-Pol $\kappa$  was recruited to the damage sites around 2–3 min after irradiation (Supplementary Fig. 1) and its accumulation persisted for over 1 h (data not shown). Notably, no CPD positive signal could be detected under the conditions used (Fig. 1D), suggesting that no major UV-photolesions were induced at the laser micro-irradiated sites. Additionally, Pol $\kappa$  accumulation at laser-induced sites of damage could be detected in G1-phase cells, suggesting that this enrichment was independent of ongoing DNA replication (Supplementary Fig. 2A). To check whether the recruitment kinetics of Pol $\kappa$  at the sites of DNA damage is similar between replicating cells and cells in G0/G1 phase, we tried to synchronize Pol $\kappa$ <sup>-/-</sup> MEFs stably reconstituted with GFP-Pol $\kappa$  and U2OS cells to G0/G1 phase through serum-starvation but failed. Later U2OS cells expressing GFP-Pol $\kappa$  were first synchronized to G2/M phase by treatment with nocodazole. Following release from the block ( $t = 0$ ), most of the cells progressed into G1 phase about 10 h later and into G1 and S phases about 15 h later (Supplementary Fig. 2B). Cells from these two time points after release were irradiated with a UVA laser and the recruitment kinetics of Pol $\kappa$  in these cells was found to be similar (Supplementary Fig. 2C & 2D). This observation hints Pol $\kappa$  may have a role beyond TLS in protecting cells from oxidative stress.

#### 3.2. The C-terminal region of Pol $\kappa$ mediates its recruitment to sites of laser-induced DNA damage

In order to examine the requirements for accumulation of Pol $\kappa$  protein in laser-irradiated cells we expressed a series of GFP-tagged truncated Pol $\kappa$  polypeptides deleted for known functional domains (Fig. 2A). As shown in Fig. 2B, GFP-tagged Pol $\kappa$  C-terminal fragments that retained the ubiquitin-binding zinc-finger motif 2 (UBZ2), a PCNA-interacting peptide (PIP), and a bipartite nuclear localization signal (NLS) accumulated Pol $\kappa$ -GFP protein within 4 min after irradiation. In contrast, GFP-Pol $\kappa$ -D1, which lacks of the C-terminal 192 amino acids and is therefore deleted for all three domains mentioned above, manifested no accumulation during a 20 min-period of observation following micro-irradiation. Identical results were obtained with GFP-Pol $\kappa$ -D4 (a.a. 650-813), in which both the NLS and PIP domains were removed. Collectively these results indicate that the C-terminal 105 amino acids of Pol $\kappa$  protein containing the UBZ2, PIP and NLS domains is sufficient for the recruitment of Pol $\kappa$  to laser-induced sites of DNA damage.

To check whether UBZ1 also functions in the recruitment of Pol $\kappa$ , we transfected cells with a Pol $\kappa$  mutant harboring a mutation in UBZ1 (D642A) [19]. We found that the recruitment of Pol $\kappa$  was reduced (Fig. 3A&B). However, this reduction was much less when compared to those provoked by mutation of either UBZ2 (D784A) or UBZs (D642A and D784A) (Fig. 3A&B). As shown in Fig. 3B, a mild defect in Pol $\kappa$  accumulation was also observed following mutation of the PIP motif (F850A and F851A), probably due to the weak binding affinity of the PIP box for PCNA [25]. Significantly, when the PIP and both UBZ domains were concurrently mutated (PIP\*: F850A and F851A; UBZ\*: D642A and D784A) no signal indicative of the accumulation of Pol $\kappa$  protein was observed (Fig. 3B), suggesting an additive effect on the accumulation.



### 3.3. MSH2 and Rad18 regulate the accumulation of Polκ to laser-induced DNA lesions

We previously reported that both the PIP and UBZs domains of Polκ are required for its optimal association with monoubiquitinated PCNA (mUb-PCNA) [19]. In light of the observation that the PIP and UBZs domains of Polκ act co-ordinately to mediate Polκ enrichment at laser-induced lesions, we speculated that mUb-PCNA may play an important role in this process. Accordingly, we treated MRC cells with H<sub>2</sub>O<sub>2</sub> a chemical known to promote the formation of DNA strand breaks, and observed that PCNA was rapidly and transiently monoubiquitinated after treatment (Fig. 4A). The level of mUb-PCNA peaked almost immediately after treatment and returned to background levels within 50 min.

It was recently reported that the mismatch repair protein MSH2 regulates the level of mUb-PCNA after exposure of cells to H<sub>2</sub>O<sub>2</sub> [18]. We asked whether deletion of the *MSH2* gene alters the accumulation of GFP-Polκ at laser-induced lesions. HCT116 (MLH1-deficient) and LoVo (MSH2-deficient) cells were transfected with GFP-Polκ plasmid and micro-irradiated with a UVA laser 24h later (Fig. 4B). Consistent with the report that a reduction of mUb-PCNA was observed in MSH2-deficient, but not in MLH1-deficient cells following H<sub>2</sub>O<sub>2</sub> treatment [18], we observed a significantly impaired assembly of Polκ in LoVo cells, but not in HCT116 cells (Fig. 4C). Notably, Polκ accumulation at laser-induced sites recovered following expression of MSH2 protein in LoVo cells (Fig. 4D). Considering that PCNA monoubiquitination after oxidative stress is Rad18-dependent, we wished to ascertain whether depletion of Rad18 would impair the recruitment of Polκ to laser-induced sites of damage. We established U2OS stable cell lines depleted of RAD18 through shRNA infection and confirmed that the monoubiquitination of PCNA was significantly reduced after UV treatment in these cells by subjecting cell extracts to western blotting with an anti-PCNA antibody (Fig. 5A). When we examined recruitment of Polκ to sites of laser-induced DNA damage, we found that the average intensity of GFP-Polκ fluorescence at damage sites was lower in RAD18-depleted cells than in control cells (Fig. 5B). Meanwhile, the proportion of RAD18-depleted cells in which Polκ was recruited to sites of micro-irradiation was also reduced (Fig. 5C). These data strongly suggested that monoubiquitinated PCNA played an important role in recruitment of Polκ to sites of laser-induced DNA damage. It was noteworthy that Rad18 knockdown cells were not completely defective for Polκ recruitment. Although the incomplete depletion of Rad18 might explain the phenomenon, other mechanisms which are independent of PCNA monoubiquitination but still require the UBD, PIP, and NLS domains might also mediate the recruitment of Polκ to the damaged sites.

### 3.4. Polκ-deficient cells are hypersensitive to hydrogen peroxide

To further elucidate the role of Polκ in oxidative damage repair we immortalized *Polκ*<sup>+/+</sup> and *Polκ*<sup>-/-</sup> MEFs and exposed the cells to H<sub>2</sub>O<sub>2</sub> or X-rays. Consistent with previously reported observations [7] *Polκ*<sup>-/-</sup> MEFs did not exhibit an enhanced sensitivity to X-rays (Fig. 6A). However, these cells were hypersensitive to H<sub>2</sub>O<sub>2</sub> treatment (Fig. 6B). To confirm that this sensitivity was directly related to the loss of Polκ in *Polκ*<sup>-/-</sup> MEFs, we stably reconstituted *Polκ*<sup>-/-</sup> MEFs with GFP-Polκ (Fig. 6C) and found that the cells became more resistant to H<sub>2</sub>O<sub>2</sub> treatment after reconstitution (Fig. 6D). To further eliminate the possibility that these results were influenced by defective repair synthesis of DNA associated with defective NER in *Polκ*<sup>-/-</sup> cells, we examined the sensitivity of *Polκ*<sup>+/+</sup>*Xpc*<sup>-/-</sup> and *Polκ*<sup>-/-</sup>*Xpc*<sup>-/-</sup> MEFs to H<sub>2</sub>O<sub>2</sub> and obtained similar results (Fig. 6E). Thus, endogenous Polκ plays a role in protecting cells from oxidative stress. To assess whether Rad18 is required for the function of Polκ in protecting cells from oxidative stress, Polκ in Rad18-depleted U2OS cells was transiently knocked down (Supplementary Fig. 3) and the sensitivity of the cells to H<sub>2</sub>O<sub>2</sub> treatment were examined. We found that knockdown of either Polκ or Rad18 made the cells more sensitive to H<sub>2</sub>O<sub>2</sub> treatment relative to the control

siRNA (Fig. 6F). No further increased sensitivity could be detected in cells depleted of both Rad18 and Pol $\kappa$ , suggesting that Pol $\kappa$  and Rad18 is epistatic for protection against oxidative stress-induced cell death.

### 3.5. Loss of Pol $\kappa$ resulted in defective repair of DNA strand breaks

We measured DNA strand break repair rates following H<sub>2</sub>O<sub>2</sub> and MMS treatments using alkaline comet assays. To avoid misinterpretations associated with the generation of strand breaks possibly associated with NER Pol $\kappa$ <sup>+/+</sup> and Pol $\kappa$ <sup>-/-</sup> cells were additionally rendered defective in NER by eliminating *XPC* function. Cells were either mock-treated or exposed to H<sub>2</sub>O<sub>2</sub> or MMS. As shown in Fig. 7A & 7B, H<sub>2</sub>O<sub>2</sub> treatment generated significant levels of strand breaks in cells. Interestingly, Pol $\kappa$ -deficient cells exhibited reduced rates of global strand break repair following H<sub>2</sub>O<sub>2</sub>-induced oxidative stress. The reduced rate of DNA strand break repair observed in Pol $\kappa$ -deficient cells within 30 min after H<sub>2</sub>O<sub>2</sub> treatment suggests a defect in SSB repair. However, given that SSBs are repaired relatively fast and we could still detect a significant difference in retained strand breakage between WT and KO cells after 3 h, it is possible that Pol $\kappa$ -deficient cells also possess a defect in DSBR. To check whether the reduced rates of chromosomal DNA strand break repair observed in Pol $\kappa$ -deficient cells following H<sub>2</sub>O<sub>2</sub> treatment was caused by loss of Pol $\kappa$ , we stably reconstituted Pol $\kappa$ <sup>-/-</sup> MEFs with GFP-Pol $\kappa$  and found that expression of GFP-Pol $\kappa$  but not GFP could effectively improve the impaired DNA repair in Pol $\kappa$ <sup>-/-</sup> MEFs (Fig. 7C). To determine the relationship between Rad18 and Pol $\kappa$  in global strand break repair after H<sub>2</sub>O<sub>2</sub> treatment, Pol $\kappa$  in Rad18-depleted U2OS cells was transiently knocked down and the rates of strand break repair were examined. We found that the levels of global strand breaks were significantly elevated in examined cells immediately after H<sub>2</sub>O<sub>2</sub> treatment (Fig. 7D). After 2 h repair incubation in drug-free medium, the extent of strand breaks almost returned to basal level in cells treated with non-targeting siRNA, while it was still high in either Pol $\kappa$  or Rad18 knockdown cells. The level of retained strand breakage in Pol $\kappa$  knockdown cells was similar to that in cells depleted of both Pol $\kappa$  and Rad18, suggesting that Pol $\kappa$  and Rad18 are epistatic for strand break repair. Remarkably, Rad18 knockdown cells manifested a lower level of retained strand breakage compared to Pol $\kappa$  and Pol $\kappa$ /Rad18 knockdown cells, indicating that partial function of Pol $\kappa$  in global strand break repair after H<sub>2</sub>O<sub>2</sub> treatment is Rad18-independent. It has been known that Pol $\kappa$ -deficient mouse embryonic stem cells and MEFs are sensitive to MMS treatment (Supplementary Fig. 4)[26]. Considering that MMS is capable of inducing DNA lesions and subsequent strand breaks [27], we further checked whether Pol $\kappa$  had a role in MMS-induced strand break repair beyond TLS. Similarly, reduced rates of global strand break repair were also observed in Pol $\kappa$ -deficient cells following MMS treatment (Fig. 7E). Collectively, these results indicated that depletion of Pol $\kappa$  compromised the repair of strand breaks.

### 3.6. Loss of Pol $\kappa$ led to defective SSB/BER and DSBR

It is known that H<sub>2</sub>O<sub>2</sub> can induce both SSBs and DSBs [28]. To directly examine whether Pol $\kappa$  can participate in SSB/BER pathway, we reconstituted the repair of G<sub>2</sub>U oligonucleotide duplex in the presence of radioactively labeled dCTP and whole-cell extracts from WT or Pol $\kappa$ -deficient MEFs as described previously[13]. Incubation of the WT cell extracts with the uracil-containing oligonucleotide duplex showed a time-dependent incorporation of  $\alpha$ -<sup>32</sup>P into the 40-mer substrate, indicating efficient BER activity in WT cells (Fig. 8A). Very intriguingly, the repair of uracil in the DNA duplex was drastically blocked in Pol $\kappa$  mutant cell extracts as indicated by diminished  $\alpha$ -<sup>32</sup>P signals (Fig. 8A). The impaired SSB/BER activity in the extracts from Pol $\kappa$ -deficient cells could be significantly improved through supplementation with purified human Pol $\kappa$ , suggesting that Pol $\kappa$  is involved in the SSB/BER pathway (Supplementary Fig. 5).

Phosphorylation of the histone variant H2AX ( $\gamma$ -H2AX) is an early step in the cellular response to DSBs and its level usually reflects the extent of DSBs. To examine whether Pol $\kappa$  can participate in repair of H<sub>2</sub>O<sub>2</sub>-induced DSBs, we compared the rate of  $\gamma$ -H2AX foci loss after H<sub>2</sub>O<sub>2</sub> treatment between Pol $\kappa$ -deficient and WT MEFs. We found that  $\gamma$ -H2AX peaked at 2 h and almost returned to background level by 6 h in WT cells (Fig. 8B). However, in the absence of Pol $\kappa$ ,  $\gamma$ -H2AX level was increased at all times and remained elevated even 10 h after removing H<sub>2</sub>O<sub>2</sub>. Therefore, loss of Pol $\kappa$  clearly impaired the repair of H<sub>2</sub>O<sub>2</sub>-induced DSBs. Notably, the basal level of  $\gamma$ -H2AX signal was higher in KO cells than in WT cells, indicating that the deletion of Pol $\kappa$  may lead to increased genomic instability.

#### 4. Discussion

Two different Pol $\kappa$  knock-out mouse strains have not revealed significant phenotypes [3]. Hence, the precise function(s) of Pol $\kappa$  *in vivo* is unclear. It is believed that the major function of Pol $\kappa$  *in vivo* is to support TLS, during which Pol $\kappa$  catalyzes the insertion of nucleotides opposite specific types of base damage in template DNA, possibly including sites of base loss (AP sites), BPDE-dG, and oxidized estrogens. Pol $\kappa$ -deficient cells are indeed hypersensitive to treatment with BPDE or estrogen derivatives [6–9].

In view of the observation that expression of mouse and human Pol $\kappa$  mRNA in the testes is confined to meiotic spermatocytes and postmeiotic spermatids (in which DNA replication is not obligatory) [29] we speculate that Pol $\kappa$  might have other unknown functions beyond TLS *in vivo*. Given that Pol $\kappa$ -deficient mice manifest elevated mutation rates in the male germline [17] and some somatic tissues [6], we postulate that Pol $\kappa$  may be involved in other DNA repair pathways required to maintain genomic stability. Since BER/SSBR has been documented to be highly efficient in extracts of male germ cells [30], we examined the possible involvement of Pol $\kappa$  in SSBR.

Our laser micro-irradiation experiments revealed that Pol $\kappa$  could be recruited to sites of laser-induced lesions in DNA and that the UBZs, NLS and PIP box of Pol $\kappa$  protein were required for its efficient accumulation at damaged sites. The requirement of NLS for Pol $\kappa$  assembly is probably due to the fact that the NLS belongs to a recently identified extended PCNA interaction surface, which is necessary for Pol $\kappa$  binding to PCNA [31]. The less requirement of the PIP box for Pol $\kappa$  recruitment to laser-induced sites of damage is consistent with the fact that this motif displays a weaker binding affinity for PCNA compared with the PIP boxes of other Y family polymerases [25]. Correspondingly, the PIP box was found to be not essential for the role of Pol $\kappa$  in replication-independent repair of DNA interstrand crosslinks [32]. Notably, the UBZs and PIP box of Pol $\kappa$  are also required for Pol $\kappa$  carrying out its functions in both TLS and NER [14,19]. Analogously, Pol $\eta$  has been documented to use the same domains to mediate its recruitment to sites of oxidative damage and UV damage [18]. It remains unknown how cells coordinate the different signals via the similar domain to finish distinct functions.

PCNA has been reported to rapidly accumulate at laser-induced sites of DNA damage [33]. The UBZs and PIP motifs are required for optimal interaction between Pol $\kappa$  and mUb-PCNA [19]. Hence, we speculated that the recruitment of Pol $\kappa$  to laser-induced lesions might be mediated through mUb-PCNA. Consistent with this notion the kinetics of the accumulation of Pol $\kappa$  at sites of damage are reminiscent of the enrichment of Rad18 (an E3 ubiquitin ligase responsible for PCNA monoubiquitination) at laser-induced DNA SSBs [34]. Furthermore, the accumulation of Pol $\kappa$  at these lesions is considerably impaired in MSH2-deficient and Rad18-depleted cells. Recently MSH2 has been reported to promote the monoubiquitination of PCNA after oxidative stress in a way that is independent of the



“canonical” MMR[18]. Also similar to Rad18 [34], the accumulation of Pol $\kappa$  at laser-induced lesions is not affected by the presence of an inhibitor of poly(ADP-ribose) polymerase or absence of XRCC1 (data not shown). These data are consistent with the previous report that PCNA monoubiquitination is independent of PARP1 and XRCC1 in response to oxidative stress [18].

The retention kinetics of Pol $\kappa$  at laser-induced sites of damage hinted that Pol $\kappa$  was also likely enriched at laser-induced DSBs based on the fact that repair proteins for SSBs and base damage dissociate very rapidly [33], while those involved in DSBR can remain at irradiated sites for more than an hour [35]. Meanwhile, Pol $\kappa$ -deficient cells were hypersensitive to H<sub>2</sub>O<sub>2</sub> and MMS treatments, which are known to generate strand breaks *in vivo*. In agreement with these observations Pol $\kappa$ -deficient cells manifested a defect in repair of H<sub>2</sub>O<sub>2</sub>- and MMS-induced global strand breaks. The overall kinetics of global strand break repair in Pol $\kappa$ -deficient cells suggested defects in both SSB/BER and DSBR. Accordingly, direct examination of the role of Pol $\kappa$  in SSB/BER confirmed a reduced activity in extracts from Pol $\kappa$  mutant cells. In addition, disappearance of  $\gamma$ -H2AX foci was significantly delayed in Pol $\kappa$ -deficient cells after H<sub>2</sub>O<sub>2</sub> treatment compared to WT cells, reflecting a defect in DSBR. Collectively, these data reveal a novel role of Pol $\kappa$  in the maintenance of genome integrity following exposure of cells to oxidative stress. Considering that Pol $\kappa$  can apparently accommodate certain bulky lesions in its catalytic core and display accurate DNA synthesis during replication of dinucleotide microsatellites [16], we speculate that Pol $\kappa$  might promote rapid repair of strand breaks in clusters or within sequences capable of forming complex secondary structures, such as microsatellite DNA [16]. In support of it, the spontaneous germline mutation rate within two expanded short tandem repeat alleles is significantly higher in Pol $\kappa$ -deficient mice compared to isogenic Pol $\kappa$  wild-type mice [17].

Since cell metabolism and environmental toxicants often introduce oxidative stress *in vivo*, the monoubiquitinated PCNA arising therefrom might recruit Pol $\kappa$  for a rapid repair of strand breaks, thereby complementing Pol $\kappa$ 's TLS function against oxidative stress. In support of it, either *REV1*<sup>-/-</sup>*Pol* $\kappa$ <sup>-/-</sup> or *REV3*<sup>-/-</sup>*Pol* $\kappa$ <sup>-/-</sup> DT 40 cells are more sensitive to MMS treatment than *REV1*<sup>-/-</sup> or *REV3*<sup>-/-</sup> cells [26]. Notably, this proposed model does not controvert the previous one in which the MMS sensitivities of Pol $\kappa$ -deficient cells are believed to be mainly attributable to the lack of TLS activity past alkylating DNA damages [26]. Further studies will be needed to explore the precise role of Pol $\kappa$  in SSB/BER and DSBR *in vivo*.

## Supplementary Material

Refer to Web version on PubMed Central for supplementary material.

## Acknowledgments

The authors thank Drs. Alan Lehmann, David Chen and Haiying Hang for cells and plasmids, Dr. Akira Yasui for helpful discussions Shiya Wang and Ana Doughty for help with initial micro-irradiation and Min Huang for preparing plasmids. This work was supported by grants 2011CB944302 & 2013CB945000 & 2012CB944702 (973 Program), 30970588 & 31170730(NSFC) (C.G), R01HL105631 (NIH) (Y.Z), 30970931 (NSFC) (T.T), KSCX2-YW-R-148 (the Knowledge Innovation Program of Chinese Academy of Sciences), 31100557 (NSFC) (H.Z), and the Chinese Academy of Sciences “One-Hundred-Talent Program” (C.G).

## References

1. Friedberg EC. Suffering in silence: the tolerance of DNA damage. *Nat Rev Mol Cell Biol.* 2005; 6:943–953. [PubMed: 16341080]

2. Yang W, Woodgate R. What a difference a decade makes: insights into translesion DNA synthesis. *Proc Natl Acad Sci U S A*. 2007; 104:15591–15598. [PubMed: 17898175]
3. Guo C, Kosarek-Stancel JN, Tang TS, Friedberg EC. Y-family DNA polymerases in mammalian cells. *Cell Mol Life Sci*. 2009; 66:2363–2381. [PubMed: 19367366]
4. Lehmann AR, Niimi A, Ogi T, Brown S, Sabbioneda S, Wing JF, Kannouche PL, Green CM. Translesion synthesis: Y-family polymerases and the polymerase switch. *DNA Repair (Amst)*. 2007; 6:891–899. [PubMed: 17363342]
5. Choi JY, Angel KC, Guengerich FP. Translesion synthesis across bulky N2-alkyl guanine DNA adducts by human DNA polymerase kappa. *J Biol Chem*. 2006; 281:21062–21072. [PubMed: 16751196]
6. Stancel JN, McDaniel LD, Velasco S, Richardson J, Guo C, Friedberg EC. Polk mutant mice have a spontaneous mutator phenotype. *DNA Repair (Amst)*. 2009; 8:1355–1362. [PubMed: 19783230]
7. Ogi T, Shinkai Y, Tanaka K, Ohmori H. Polkappa protects mammalian cells against the lethal and mutagenic effects of benzo[a]pyrene. *Proc Natl Acad Sci U S A*. 2002; 99:15548–15553. [PubMed: 12432099]
8. Mizutani A, Okada T, Shibutani S, Sonoda E, Hochegger H, Nishigori C, Miyachi Y, Takeda S, Yamazoe M. Extensive chromosomal breaks are induced by tamoxifen and estrogen in DNA repair-deficient cells. *Cancer Res*. 2004; 64:3144–3147. [PubMed: 15126352]
9. Bi X, Slater DM, Ohmori H, Vaziri C. DNA polymerase kappa is specifically required for recovery from the benzo[a]pyrene-dihydrodiol epoxide (BPDE)-induced S-phase checkpoint. *J Biol Chem*. 2005; 280:22343–22355. [PubMed: 15817457]
10. Lehmann AR. New functions for Y family polymerases. *Mol Cell*. 2006; 24:493–495. [PubMed: 17188030]
11. Seki M, Gearhart PJ, Wood RD. DNA polymerases and somatic hypermutation of immunoglobulin genes. *EMBO Rep*. 2005; 6:1143–1148. [PubMed: 16319960]
12. McIlwraith MJ, Vaisman A, Liu Y, Fanning E, Woodgate R, West SC. Human DNA polymerase eta promotes DNA synthesis from strand invasion intermediates of homologous recombination. *Mol Cell*. 2005; 20:783–792. [PubMed: 16337601]
13. Petta TB, Nakajima S, Zlatanou A, Despras E, Couve-Privat S, Ishchenko A, Sarasin A, Yasui A, Kannouche P. Human DNA polymerase iota protects cells against oxidative stress. *Embo J*. 2008; 27:2883–2895. [PubMed: 18923427]
14. Ogi T, Limsirichaikul S, Overmeer RM, Volker M, Takenaka K, Cloney R, Nakazawa Y, Niimi A, Miki Y, Jaspers NG, Mullenders LH, Yamashita S, Foustari MI, Lehmann AR. Three DNA polymerases, recruited by different mechanisms, carry out NER repair synthesis in human cells. *Mol Cell*. 2010; 37:714–727. [PubMed: 20227374]
15. Schenten D, Gerlach VL, Guo C, Velasco-Miguel S, Hladik CL, White CL, Friedberg EC, Rajewsky K, Esposito G. DNA polymerase kappa deficiency does not affect somatic hypermutation in mice. *Eur J Immunol*. 2002; 32:3152–3160. [PubMed: 12555660]
16. Hile SE, Wang X, Lee MY, Eckert KA. Beyond translesion synthesis: polymerase kappa fidelity as a potential determinant of microsatellite stability. *Nucleic Acids Res*. 2012; 40:1636–1647. [PubMed: 22021378]
17. Burr KL, Velasco-Miguel S, Duvvuri VS, McDaniel LD, Friedberg EC, Dubrova YE. Elevated mutation rates in the germline of Polkappa mutant male mice. *DNA Repair (Amst)*. 2006; 5:860–862. [PubMed: 16731053]
18. Zlatanou A, Despras E, Braz-Petta T, Boubakour-Azzouz I, Pouvelle C, Stewart GS, Nakajima S, Yasui A, Ishchenko AA, Kannouche PL. The hMsh2-hMsh6 complex acts in concert with monoubiquitinated PCNA and Pol eta in response to oxidative DNA damage in human cells. *Mol Cell*. 2011; 43:649–662. [PubMed: 21855803]
19. Guo C, Tang TS, Bienko M, Dikic I, Friedberg EC. Requirements for the interaction of mouse Polkappa with ubiquitin and its biological significance. *J Biol Chem*. 2008; 283:4658–4664. [PubMed: 18162470]
20. Cheo DL, Ruven HJ, Meira LB, Hammer RE, Burns DK, Tappe NJ, van Zeeland AA, Mullenders LH, Friedberg EC. Characterization of defective nucleotide excision repair in XPC mutant mice. *Mutat Res*. 1997; 374:1–9. [PubMed: 9067411]

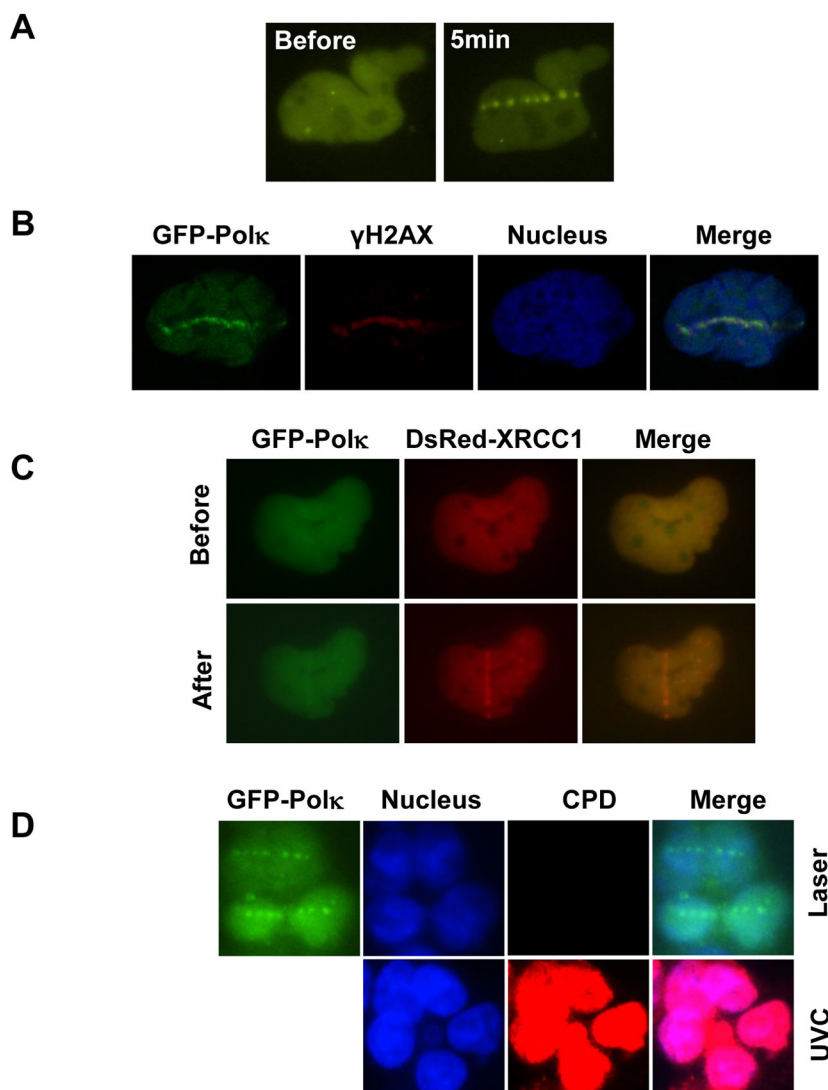
21. Guo C, Tang TS, Bienko M, Parker JL, Bielen AB, Sonoda E, Takeda S, Ulrich HD, Dikic I, Friedberg EC. Ubiquitin-binding motifs in REV1 protein are required for its role in the tolerance of DNA damage. *Mol Cell Biol.* 2006; 26:8892–8900. [PubMed: 16982685]
22. Uematsu N, Weterings E, Yano K, Morotomi-Yano K, Jakob B, Taucher-Scholz G, Mari PO, van Gent DC, Chen BP, Chen DJ. Autophosphorylation of DNA-PKCS regulates its dynamics at DNA double-strand breaks. *J Cell Biol.* 2007; 177:219–229. [PubMed: 17438073]
23. Guo C, Sonoda E, Tang TS, Parker JL, Bielen AB, Takeda S, Ulrich HD, Friedberg EC. REV1 protein interacts with PCNA: significance of the REV1 BRCT domain in vitro and in vivo. *Mol Cell.* 2006; 23:265–271. [PubMed: 16857592]
24. Zou J, Chen Q, Tang S, Jin X, Chen K, Zhang T, Xiao X. Olaquinox-induced genotoxicity and oxidative DNA damage in human hepatoma G2 (HepG2) cells. *Mutat Res.* 2009; 676:27–33. [PubMed: 19486861]
25. Hishiki A, Hashimoto H, Hanafusa T, Kamei K, Ohashi E, Shimizu T, Ohmori H, Sato M. Structural basis for novel interactions between human translesion synthesis polymerases and proliferating cell nuclear antigen. *J Biol Chem.* 2009; 284:10552–10560. [PubMed: 19208623]
26. Takenaka K, Ogi T, Okada T, Sonoda E, Guo C, Friedberg EC, Takeda S. Involvement of vertebrate Polkappa in translesion DNA synthesis across DNA monoalkylation damage. *J Biol Chem.* 2006; 281:2000–2004. [PubMed: 16308320]
27. Fortini P, Pascucci B, Belisario F, Dogliotti E. DNA polymerase beta is required for efficient DNA strand break repair induced by methyl methanesulfonate but not by hydrogen peroxide. *Nucleic Acids Res.* 2000; 28:3040–3046. [PubMed: 10931918]
28. Kryston TB, Georgiev AB, Pissis P, Georgakilas AG. Role of oxidative stress and DNA damage in human carcinogenesis. *Mutat Res.* 2011; 711:193–201. [PubMed: 21216256]
29. Velasco-Miguel S, Richardson JA, Gerlach VL, Lai WC, Gao T, Russell LD, Hladik CL, White CL, Friedberg EC. Constitutive and regulated expression of the mouse Dinb (Polkappa) gene encoding DNA polymerase kappa. *DNA Repair (Amst).* 2003; 2:91–106. [PubMed: 12509270]
30. Olsen AK, Bjortuft H, Wiger R, Holme J, Seeberg E, Bjoras M, Brunborg G. Highly efficient base excision repair (BER) in human and rat male germ cells. *Nucleic Acids Res.* 2001; 29:1781–1790. [PubMed: 11292851]
31. Bienko M, Green CM, Sabbioneda S, Crosetto N, Matic I, Hibbert RG, Begovic T, Niimi A, Mann M, Lehmann AR, Dikic I. Regulation of translesion synthesis DNA polymerase eta by monoubiquitination. *Mol Cell.* 2010; 37:396–407. [PubMed: 20159558]
32. Williams HL, Gottesman ME, Gautier J. Replication-independent repair of DNA interstrand crosslinks. *Mol Cell.* 2012; 47:140–147. [PubMed: 22658724]
33. Lan L, Nakajima S, Oohata Y, Takao M, Okano S, Masutani M, Wilson SH, Yasui A. In situ analysis of repair processes for oxidative DNA damage in mammalian cells. *Proc Natl Acad Sci U S A.* 2004; 101:13738–13743. [PubMed: 15365186]
34. Nakajima S, Lan L, Kanno S, Usami N, Kobayashi K, Mori M, Shiomi T, Yasui A. Replication-dependent and -independent responses of RAD18 to DNA damage in human cells. *J Biol Chem.* 2006; 281:34687–34695. [PubMed: 16980296]
35. Kim JS, Krasieva TB, Kurumizaka H, Chen DJ, Taylor AM, Yokomori K. Independent and sequential recruitment of NHEJ and HR factors to DNA damage sites in mammalian cells. *J Cell Biol.* 2005; 170:341–347. [PubMed: 16061690]

### Highlights

Pol $\kappa$  accumulates at laser-induced sites of damage via its C-terminus.

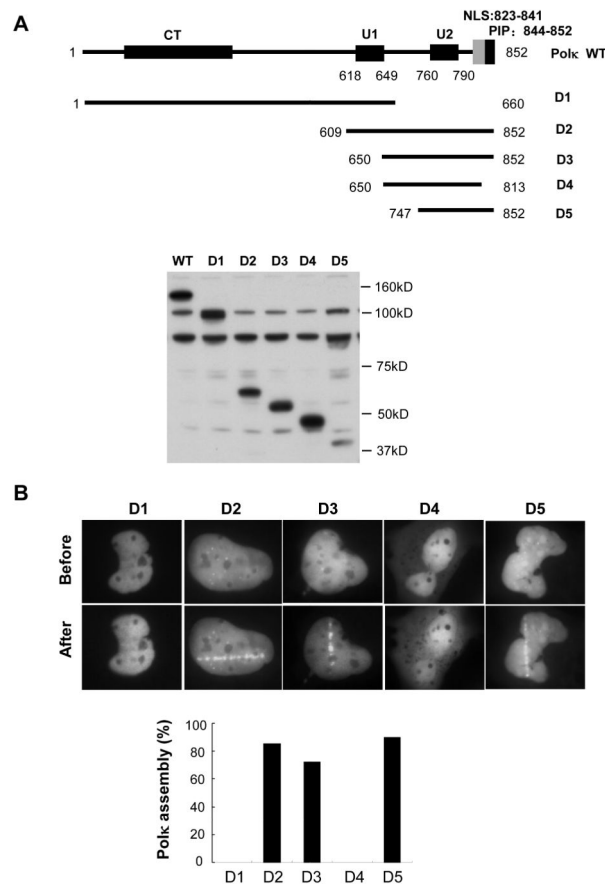
The MSH2- and Rad18-dependent monoubiquitinated PCNA is required for efficient Pol $\kappa$  accumulation.

Pol $\kappa$ -deficient MEFs are sensitive to H<sub>2</sub>O<sub>2</sub> treatment and have a defect in single-strand break repair and double strand break repair.



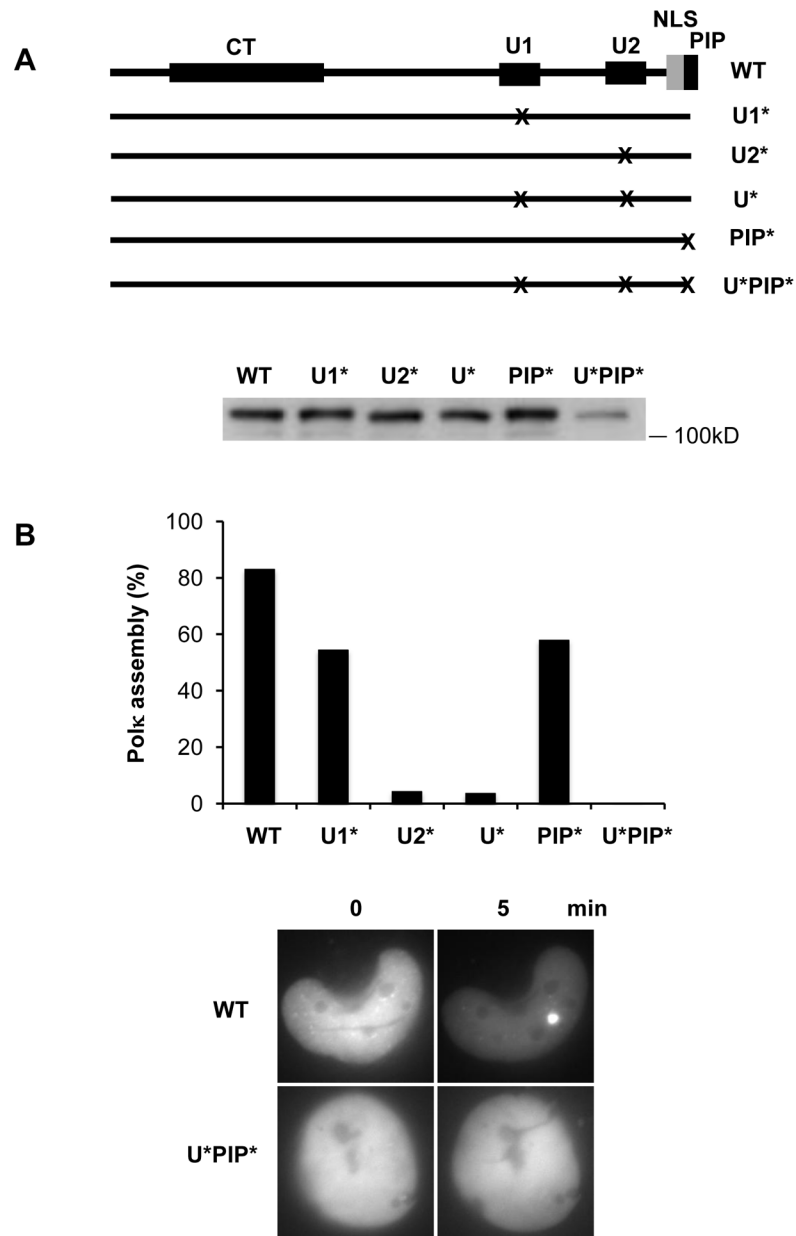
**Figure 1.** Accumulation of GFP-Pol $\kappa$  at laser-induced DNA damage sites. (A) MRC5 cells transfected with GFP-Pol $\kappa$  were micro-irradiated with laser. 5 min later, the cell images were recorded. (B) MRC5 cells transfected with GFP-Pol $\kappa$  were micro-irradiated with laser (72% output). 45 min later, the cells were fixed and stained with antibodies to  $\gamma$ -H2AX. Nuclei were co-stained with DRAQ5. (C) MRC5 cells transfected with GFP-Pol $\kappa$  and DsRed-XRCC1 were micro-irradiated with laser (58% output). 5 min later, the cell images were captured. (D) No CPD lesions were detected at the laser micro-irradiated sites under the conditions for GFP-Pol $\kappa$  accumulation. Top panel: HCT116 cells expressing GFP-Pol $\kappa$  were treated as in B. Bottom Panel: HCT116 cells were irradiated with 10J/m<sup>2</sup> UVC. After fixation, the cells were denatured with HCl and then incubated with anti-CPDs antibodies according to the manufacturer's protocol. CPD signals were only detected in UV-irradiated cells but not in laser micro-irradiated cells.





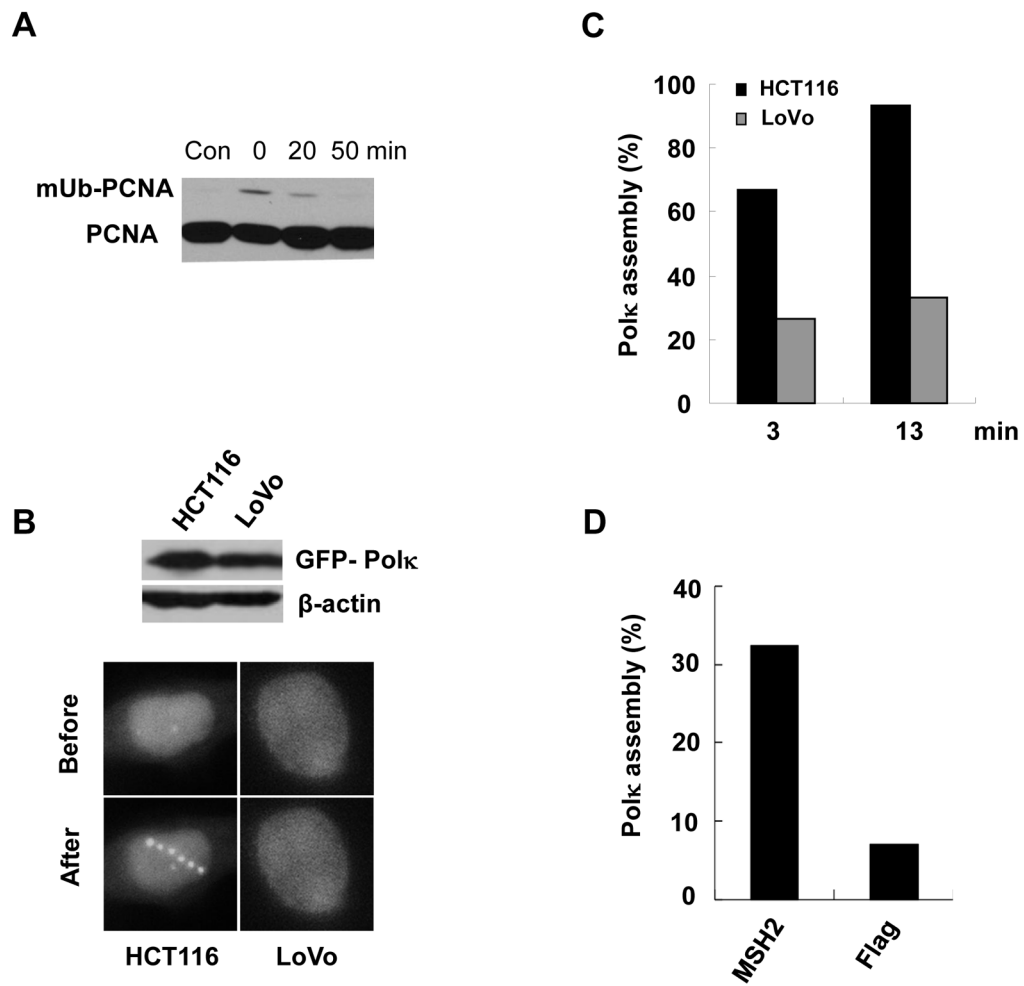
**Figure 2.**

The C-terminus of Pol $\kappa$  mediated its recruitment to laser-induced DNA damage sites. (A) Top panel: Schematic representation of Pol $\kappa$  domains: U1, ubiquitin-binding zinc finger 1 (residues 618–649); U2, ubiquitin-binding zinc finger 2 (residues 760–790); NLS, nuclear localization signal (residues 823–841); PIP, PCNA-interacting peptide (residues 844–852) and Pol $\kappa$  deletion (D1, D2, D3, D4, and D5). Bottom Panel: MRC5 cells expressing various GFP-Pol $\kappa$  constructs were harvested and extracts were separated by SDS-PAGE, and incubated with anti-GFP antibodies. (B) MRC5 cells transfected with a series of truncated GFP-Pol $\kappa$  were micro-irradiated. The cell images were recorded before and after micro-irradiation (Top panel). The percentage of GFP-Pol $\kappa$ -expressing cells in which the protein was localized at the sites of damage was determined (Bottom panel).



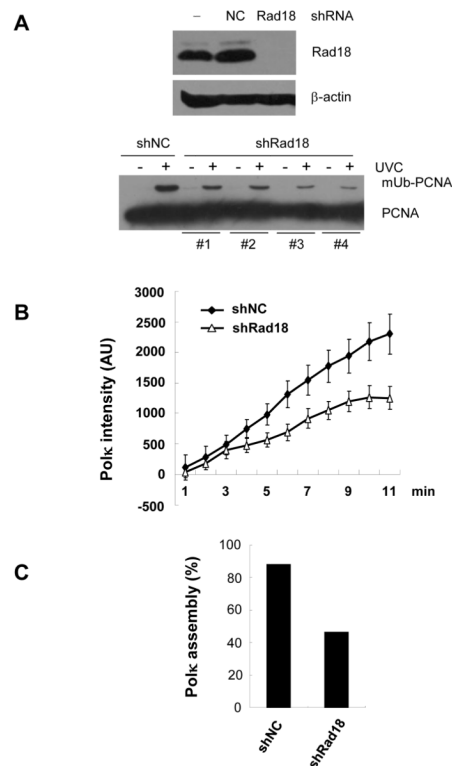
**Figure 3.**

The UBZs and PIP motifs of Polκ were required for its efficient accumulation at laser-induced DNA damage sites. (A) Top panel: Schematic representation of Polκ point mutants: U1\* (D642A), U2\* (D784A), U\* (D642A and D784A), PIP\* (F850A and F851A), and U\*PIP\* (D642A, D784A, F850A and F851A). The X represents point mutation introduced in the UBZ or PIP of Polκ sequence. Bottom Panel: MRC5 cells expressing various GFP-Polκ constructs were harvested and extracts were separated by SDS-PAGE, and incubated with anti-GFP antibodies. (B) MRC5 cells expressing various GFP-Polκ mutants were micro-irradiated and the percentage of GFP-Polκ-expressing cells in which the protein was localized at the sites of damage was determined. Bottom panel: Representative images are shown for cells transfected with pGFP-Polκ WT or U\*PIP\*.

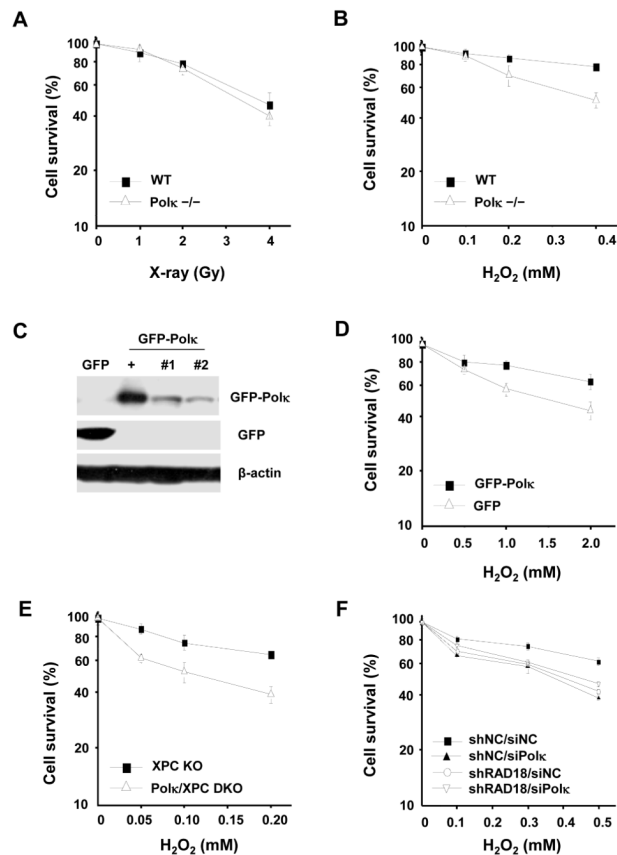


**Figure 4.**

MSH2-deficient cells exhibited an impaired GFP-Pol $\kappa$  recruitment at laser-induced sites of damage. (A) MRC5 cells were treated with 0.5mM H<sub>2</sub>O<sub>2</sub> at 4°C for about 60min. Then the triton-insoluble fractions were harvested at indicated time-points. The levels of mUb-PCNA were detected by immunoblotting with anti-PCNA antibody. (B) HCT116 and LoVo cells were transfected with GFP-Pol $\kappa$ . 24h later, the cells were micro-irradiated with a UVA laser. 2 min later, the cell images were captured (Bottom panel). Top Panel: HCT116 and LoVo cells expressing GFP-Pol $\kappa$  construct were harvested and extracts were separated by SDS-PAGE, and incubated with anti-GFP antibodies. (C) Quantification of HCT116 and LoVo cells with GFP-Pol $\kappa$  accumulations at the indicated time points after laser micro-irradiation. (D) LoVo cells were co-transfected with GFP-Pol $\kappa$  and Flag-MSH2. 24h later, the cells were micro-irradiated with a UVA laser and Pol $\kappa$  accumulation was quantified as in (C).

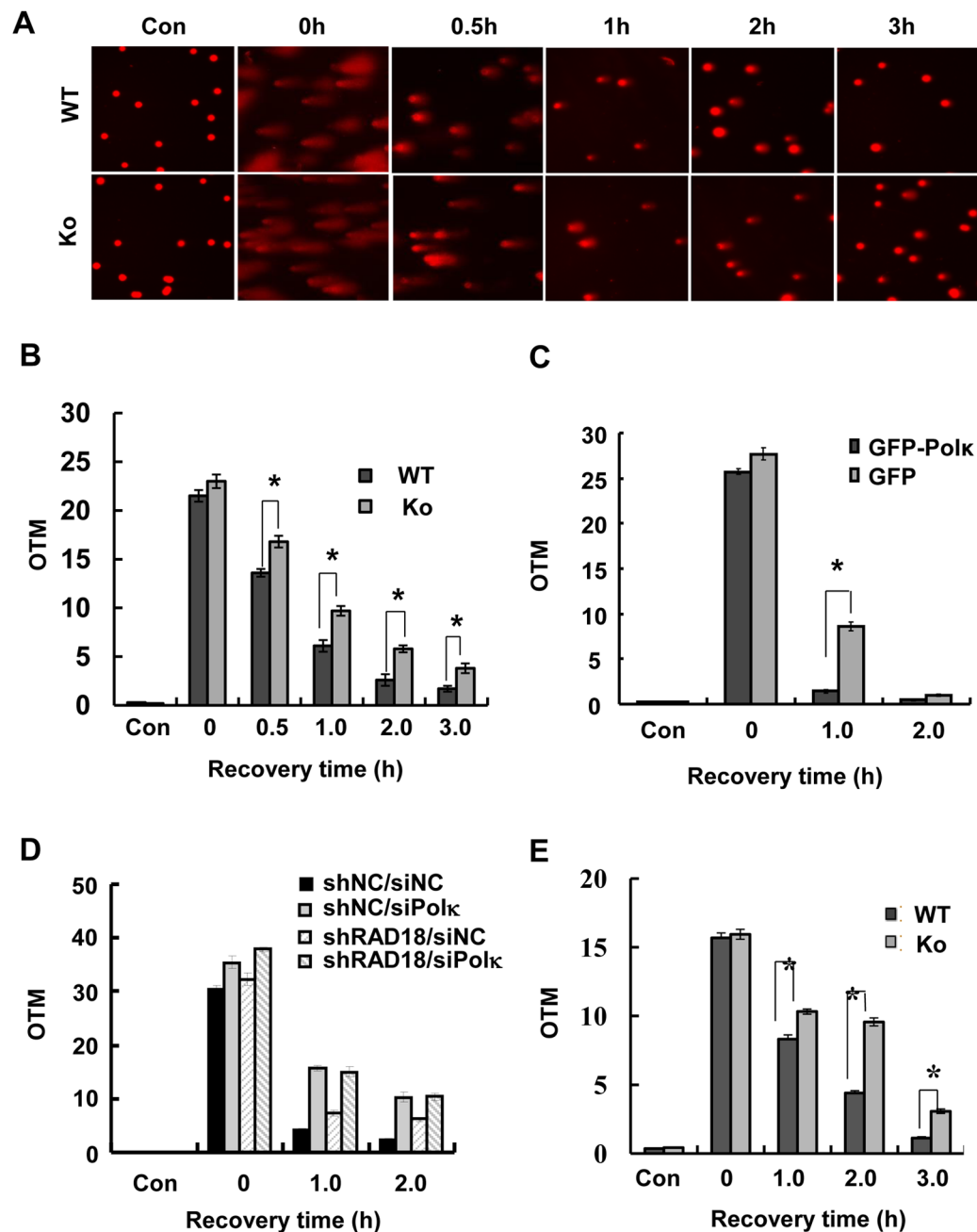


**Figure 5.** Knockdown of Rad18 decreased GFP-Pol $\kappa$  recruitment at laser-induced sites of damage. A) U2OS cells were transfected with shRad18 or shNC and stable cell lines with a reduced Rad18 level were established. Top panel: western blot to show the level of Rad18 in stable cells. Bottom: U2OS cells-depleted of Rad18 were UV irradiated and cell extracts were separated by SDS-PAGE, and incubated with anti-PCNA antibodies. (B) The indicated stable cells were transfected with GFP-Pol $\kappa$ . 24h later, the cells were micro-irradiated with a UVA laser and kinetic analysis of GFP-Pol $\kappa$  intensity at laser-irradiated sites was performed. Error bars represent standard errors based on 10 independent measurements. C) The proportion of cells with Pol $\kappa$  accumulation was quantified.

**Figure 6.**

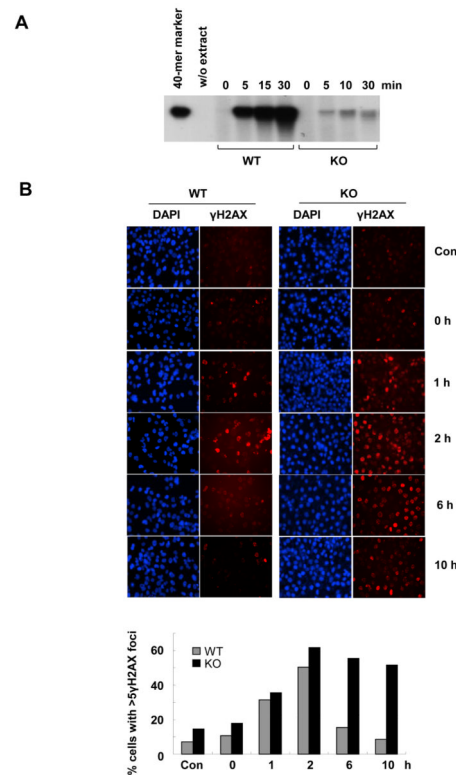
The sensitivity of Polκ-deficient MEFs to DNA damage agent H<sub>2</sub>O<sub>2</sub>. Polκ<sup>-/-</sup> MEFs were treated with X-rays (A) or H<sub>2</sub>O<sub>2</sub> at 4°C for 1 h (B) and further incubated in fresh medium for 7–10 days. (C) Cell lysates of Polκ<sup>-/-</sup> MEFs complemented with GFP or GFP-Polκ were separated by SDS-PAGE and then incubated with anti-GFP or anti-β-actin antibodies. “+” represents a positive control. “#1” and “#2” are two different stable clones. (D) Polκ<sup>-/-</sup> MEFs complemented with GFP or GFP-Polκ were treated with H<sub>2</sub>O<sub>2</sub> at 4°C for 1 h and further incubated in fresh medium for 7–10 days. (E) Polκ and XPC double knockout MEFs were treated with H<sub>2</sub>O<sub>2</sub> as in (D). (F) Polκ in Rad18-depleted U2OS cells was transiently knocked down and the sensitivity of the cells to H<sub>2</sub>O<sub>2</sub> treatment were examined as in (D). Surviving fraction was expressed as a percentage of mock-treated cells. Values are the mean of three independent experiments (+/- SE).



**Figure 7.**

Loss of Polκ resulted in reduced rates of global strand break repair. (A) *Polκ*<sup>+/+</sup>*Xpc*<sup>-/-</sup> and *Polκ*<sup>-/-</sup>*Xpc*<sup>-/-</sup> MEFs were treated with 200 μM H<sub>2</sub>O<sub>2</sub> for 10 min. At indicated time points cells were analyzed with alkaline comet assay. Representative images of cells for each time point are shown. (B) The quantitative distribution of tail moments for each time point is shown. (C) *Polκ*<sup>-/-</sup> MEFs complemented with GFP or GFP-Polκ were treated with 600 μM H<sub>2</sub>O<sub>2</sub> at 4°C for 30 min. (D) Rad18-depleted U2OS cells were transfected with siPolκ, 48 h later, the cells were treated with 1 mM H<sub>2</sub>O<sub>2</sub> at 4°C for 10 min. (E) *Polκ*<sup>+/+</sup>*Xpc*<sup>-/-</sup> and *Polκ*<sup>-/-</sup>*Xpc*<sup>-/-</sup> MEFs were treated with 300 μM MMS for 1h. At indicated time points cells were analyzed with alkaline comet assay. The quantitative distribution of tail moments

for each time point is shown. At least 100 cells were scored in each sample and experiment. Data represent the mean of three independent experiments ( $\pm$  SE).

**FIG. 8.**

Loss of Polκ resulted in defects in SSBR and DSBR. (A) SSBR/BER activity was reduced in extracts from Polκ mutant cells. Denaturing gel of G\_U repair products after incubation with the whole-cell extracts from WT or Polκ-deficient MEFs: 4nM of G\_U was incubated with 10μg extract at 37°C, and aliquots were withdrawn at different time intervals and analysed on a 10% denaturing PAGE. (B) γ-H2AX foci persisted much longer in Polκ-deficient cells than in WT cells after H<sub>2</sub>O<sub>2</sub> treatment. WT and Polκ-deficient MEFs were treated with 0.5mM H<sub>2</sub>O<sub>2</sub> at 4°C for 10min. At indicated time points the cells were fixed and stained with anti-γ-H2AX and DAPI. Top panel: Visualization of γ-H2AX foci (red) and DNA (blue) in WT and Polκ-deficient cells. Bottom panel: Percentage of cells with over γ-H2AX foci. Significantly higher numbers of KO cells are foci positive relative to WT cells at 6 h and 8 h ( $p < 0.001$ ).